



HAL
open science

Experimental study and numerical simulation of high temperature (1100–1250 °C) oxidation of prior-oxidized zirconium alloy

Benoît Mazères, Clara Desgranges, Caroline Toffolon-Mascret, Daniel Monceau

► To cite this version:

Benoît Mazères, Clara Desgranges, Caroline Toffolon-Mascret, Daniel Monceau. Experimental study and numerical simulation of high temperature (1100–1250 °C) oxidation of prior-oxidized zirconium alloy. *Corrosion Science*, 2016, 103, pp.10-19. 10.1016/j.corsci.2015.10.018 . hal-02429044

HAL Id: hal-02429044

<https://hal.science/hal-02429044>

Submitted on 6 Jan 2020

HAL is a multi-disciplinary open access archive for the deposit and dissemination of scientific research documents, whether they are published or not. The documents may come from teaching and research institutions in France or abroad, or from public or private research centers.

L'archive ouverte pluridisciplinaire **HAL**, est destinée au dépôt et à la diffusion de documents scientifiques de niveau recherche, publiés ou non, émanant des établissements d'enseignement et de recherche français ou étrangers, des laboratoires publics ou privés.



Open Archive Toulouse Archive Ouverte (OATAO)

OATAO is an open access repository that collects the work of Toulouse researchers and makes it freely available over the web where possible

This is an author's version published in: <http://oatao.univ-toulouse.fr/24463>

Official URL: <https://doi.org/10.1016/j.corsci.2015.10.018>

To cite this version:

Mazères, Benoît  and Desgranges, Clara and Toffolon-Masclet, Caroline and Monceau, Daniel  *Experimental study and numerical simulation of high temperature (1100–1250 °C) oxidation of prior-oxidized zirconium alloy.* (2016) *Corrosion Science*, 103. 10-19. ISSN 0010-938X

Any correspondence concerning this service should be sent to the repository administrator: tech-oatao@listes-diff.inp-toulouse.fr

Experimental study and numerical simulation of high temperature (1100–1250 °C) oxidation of prior-oxidized zirconium alloy

Benoît Mazères^{a,d}, Clara Desgranges^{b,*}, Caroline Toffolon-Masclét^c, Daniel Monceau^d

^a CEA, DEN, DPC, SCCME, Laboratoire d'Etude de la Corrosion Non Aqueuse, Gif-Sur-Yvette, F-91191, France

^b CEA, DEN, DPC, SCCME, Laboratoire Modélisation, Thermodynamique et Thermochimie, Gif-Sur-Yvette, F-91191, France

^c CEA, DEN, DMN, SRMA, Laboratoire d'Analyse Microstructurale des Matériaux, Gif-Sur-Yvette, F-91191, France

^d CIRIMAT, Université de Toulouse, ENSIACET, 4 Allée Emile Monso, BP 44362, F-31030 Toulouse Cedex 4, France

ARTICLE INFO

Keywords:

- A. alloy
- A. zirconium
- B. modelling studies
- C. high-temperature oxidation
- C. oxygen diffusion

ABSTRACT

Previous experiments showed that the thickness of a thick prior-oxide layer formed on Zircaloy-4 fuel cladding can decrease during the first seconds at very high-temperature, before re-growing. We confirmed these results with oxidations performed at 1200 °C on prior-oxidized Zircaloy-4. The initial reduction of the prior-oxide was explained by the balance of the oxygen fluxes at the metal/oxide interface and successfully reproduced by numerical simulations using a diffusion-reaction model. Different hypotheses were considered for the diffusion coefficients of oxygen in the different layers. This allowed discussing the effect of the prior-oxidation on the kinetics of oxygen embrittlement of the metallic substrate.

1. Introduction

Zirconium alloys (such as Zircaloy-4) are widely used as fuel cladding tubes in nuclear Pressurized-light-Water-Reactors. In service conditions, fuel cladding tubes are in contact with the water of the primary circuit of PWR at a temperature close to 320 °C and under an isostatic pressure of 1.55.10⁷ Pa. This leads to the formation of a layer of zirconia on the external surface of the fuel cladding tubes. On Zircaloy-4 claddings, after the whole life of fuel cladding tubes (four cycles of irradiation) in a PWR, the maximum

thickness of this zirconia layer is about 100 μm. This oxide layer has to be carefully considered in safety studies, especially in the case of a hypothetical scenario of loss-of-coolant-accident. In this scenario, fuel cladding tubes could undergo a high temperature oxidation ($T \approx 1200$ °C) in water steam for a maximum duration of a few minutes [1]. This high temperature oxidation would induce the formation of a significant thickness of zirconia and the diffusion of oxygen into the fuel cladding tube [1–6]. Chuto et al. [4], Guilbert et al. [5] and Le Saux et al. [1] performed oxidation treatments at high temperature on prior-oxidized zirconium alloy. Prior-oxidized samples were chosen in order to simulate the layer of zirconia formed in-service.¹ During the first seconds of the high temperature treatment, the authors have noticed a reduction of the thickness of the prior-oxide layer, in the case of a thick prior-oxide, before the re-growth of a new additional layer of zirconia at the metal/oxide interface. This initial reduction of the thickness of prior-oxide can be explained by the oxygen flux balance at the metal/oxide interface [6]. At the beginning of the high tempera-

Abbreviations: α_{red} , $\alpha_{Zr}(O)$ phase formed by reduction of the low temperature oxide layer; Exp, experimental, i.e. data link with experimental results; EKINOX-Zr, Estimation KINetics OXidation numerical model for Zr alloys; HCP, hexagonal close-packed; HT, high temperature; HTox/HT ZrO₂, oxide layer formed at high temperature ($T \geq 1000$ °C); LOCA, loss-of-coolant-accident; LT, Low temperature, i.e. the in-service temperature of the PWR ($T \approx 320$ °C); LTox/LT ZrO₂, oxide layer formed at low temperature; Num., numerical, i.e. data link to numerical results; PBR, Pilling–Bedworth ratio; Prior- β_{Zr} , phase formed from the cooling of β_{Zr} phase stable at high temperature; PWR, pressurized-light-water-reactor.

* Corresponding author. Fax: +33 1 69 08 92 21.

E-mail addresses: benoit.mazeres@ensiacet.fr (B. Mazères), clara.desgranges@cea.fr (C. Desgranges), caroline.toffolon@cea.fr (C. Toffolon-Masclét), daniel.monceau@ensiacet.fr (D. Monceau).

¹ Chuto used samples after irradiation in PWR, Guilbert et al. used samples prior-oxidized in pure oxygen at 425 °C and Le Saux et al. used samples prior-oxidized in autoclave at 360 °C and under 1.90.10⁷ Pa in water with addition of B and Li to simulate the PWR chemistry.

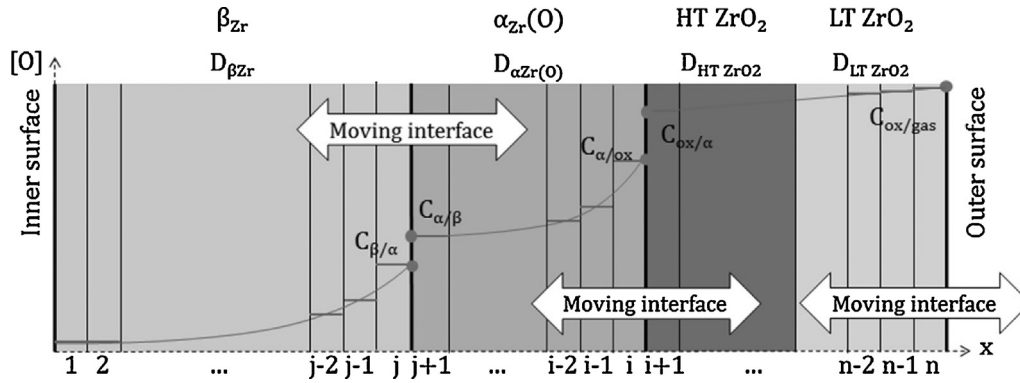


Fig. 1. Schematic of the EKINOX-Zr model.

ture treatment, because of the very high solubility of oxygen in $\alpha_{Zr}(O)$ phase at these temperatures, the gradient of the activity of oxygen in the $\alpha_{Zr}(O)$ layer is high, whereas the oxygen activity gradient is rather low in the thick layer of prior-oxide. Consequently, the inward flux of oxygen in the oxide is lower than the inward flux in the $\alpha_{Zr}(O)$ phase. Hence, the balance of the fluxes at the metal/oxide interface leads to the reduction of the prior-oxide despite the oxidizing atmosphere. This also leads to the growth of an $\alpha_{Zr}(O)$ phase at the metal/oxide interface. The flux of oxygen in the $\alpha_{Zr}(O)$ layer decreases with its thickening, i.e. with time, whereas the inward flux of oxygen in the oxide layer increases with the decrease of its thickness. Hence, after a certain time, the balance of the fluxes of oxygen at the metal/oxide interface reverses and the new oxide starts growing. In a previous work EKINOX-Zr model calculations have been used to reproduce this particular diffusion path [7]. These calculations were based on a 1D numerical resolution of diffusion-reaction equations describing the diffusion of oxygen in the $ZrO_2/\alpha_{Zr}(O)/\beta_{Zr}$ system. It was shown that the experimental data cannot be exactly reproduced by simulations done with the assumption of a unique and constant coefficient of diffusion of oxygen in each of the three phases. The aim of this paper is to understand the influence of a layer of prior-oxide² on the diffusion of oxygen in the metallic matrix during oxidation at high temperature. To do so, experiments at high temperatures were performed on prior-oxidized Zircaloy-4 samples and several hypotheses were tested using EKINOX-Zr to evaluate their validity and consequences.

2. Numerical model EKINOX-Zr

2.1. General description

The numerical tool EKINOX-Zr [6–8] was designed to simulate the oxidation at high temperature of zirconium alloys. The kinetics of growth of both the oxide scale and the layer of $\alpha_{Zr}(O)$ phase were calculated. A numerical resolution of Fick's equations with boundary conditions on moving interfaces allowed determining the profiles of diffusion of oxygen. The interfaces were considered at the local equilibrium and the thermodynamic database Zircobase [9] was used to calculate the interfacial concentrations. In the model, the fuel cladding tube was modeled as a one-dimensional planar domain. Fig. 1 presents a schematic of EKINOX-Zr model, with the

assumption that one layer of each phase (ZrO_2 , $\alpha_{Zr}(O)$ and β_{Zr}) coexist from the very beginning of the simulation.

The fuel cladding tube is divided into n slabs. In each slab of metal, a concentration of oxygen X_O^p is defined. In the same way, $X_{V_o}^q$ is the concentration of anionic vacancies defined in each slab of the oxide layer. Following the Wagner's theory of oxidation [10], the transport of oxygen is calculated from slab to slab using an explicit treatment of the fluxes of oxygen in the metal (Eq. (1)) and of the fluxes of anionic vacancies in the oxide (Eq. (2)).

$$\forall p \in [1; i] \quad J_O^p = -\frac{D_O^p}{\Omega^p} \times \frac{X_O^{p+1} - X_O^p}{\frac{1}{2}(e^p + e^{p+1})} \quad (\text{metal}) \quad (1)$$

$$\forall q \in [i+1; n] \quad J_{V_o}^q = -\frac{(1+z)D_{V_o}^q}{\Omega^q} \times \frac{X_{V_o}^{q+1} - X_{V_o}^q}{\frac{1}{2}(e^q + e^{q+1})} \quad (\text{oxide}) \quad (2)$$

Thus, the balance of fluxes in each slab leads to a variation of the concentration of oxygen (Eq. (3), in the metal) or of the concentration of vacancies (Eq. (4), in the oxide) in each slab.

$$\forall p \in [1; i] \quad \frac{dX_O^p}{dt} = \Omega^p \times \frac{J_O^p - J_O^{p+1}}{e^p} \quad (\text{metal}) \quad (3)$$

$$\forall q \in [i+1; n] \quad \frac{dX_{V_o}^q}{dt} = \Omega^q \times \frac{J_{V_o}^q - J_{V_o}^{q+1}}{e^q} \quad (\text{oxide}) \quad (4)$$

The displacement of the metal/oxide interface is numerically achieved by introducing equations describing the variations of the thickness of the slab for the two slabs i and $i+1$ close to the interface. These variations are governed by the difference in fluxes of oxygen at either side of the interface (Eqs. (5) and (6)). The displacement of the $\alpha_{Zr}(O)/\beta_{Zr}$ interface is calculated with the same procedure (Eqs. (7) and (8)).

$$\frac{de^{i+1}}{dt} = \frac{P\Omega}{\gamma} \times \frac{J_{V_o}^{i-1} - J_{V_o}^{i+1}}{C_{ox/\alpha_{Zr}(O)} - C_{\alpha_{Zr}(O)/ox}} \quad (5)$$

$$\frac{de^i}{dt} = -P \frac{de^{i+1}}{dt} \quad (6)$$

$$\frac{de^{j+1}}{dt} = \Omega \frac{J_O^{j-1} - J_O^{j+1}}{C_{\alpha_{Zr}(O)/\beta_{Zr}} - C_{\beta_{Zr}/\alpha_{Zr}(O)}} \quad (7)$$

$$\frac{de^j}{dt} = -\frac{de^{j+1}}{dt} \quad (8)$$

The boundary conditions are given in Eqs. (9) and (10). A mirror condition is set in the slab 1 (Eq. (10)). Hence, in order to simulate the oxidation on one side or on the two sides (inside and outside) of the fuel cladding tube, the total number of slabs is attributed to

² In the rest of this article, the oxide layer formed during in-service condition will be mentioned as « prior-oxide layer » or « LT oxide layer » (LT—low temperature, i.e. in-service conditions of PWR).

represent respectively the total thickness of the whole of the fuel cladding tube or half of it.

$$\frac{dX_{V_0}^n}{dt} = \frac{J_{V_0}^{n-1}}{e^n} \quad (9)$$

$$\frac{dX_0^1}{dt} = \frac{J_0^2}{e^1} \quad (10)$$

The concentrations of oxygen at the $\alpha_{Zr}(O)/\beta_{Zr}$ interface and at the metal/oxide interface are considered at thermodynamic equilibrium (Eqs. (11) and (12)). EKINOX-Zr has been coupled with the thermodynamic database Zircobase [9]. In practice, the chemical parameters of the system (temperature, composition and pressure) describing the local concentration at each interface are calculated by EKINOX-Zr from the step of integration of the diffusion and sent as input parameters to ThermoCalc software thanks to TQ interface.³ ThermoCalc calculates the equilibrium concentrations which are implemented backward as boundaries conditions at oxide/metal (i.e. oxide/ $\alpha_{Zr}(O)$) and $\alpha_{Zr}(O)/\beta_{Zr}$ interfaces [8].

$$X_{V_0}^n t = [V_0]_{ox/gas}; X_{V_0}^{i+1} t = [V_0]_{ox/\alpha_{Zr}O} \quad (11)$$

$$X_0^i(t) = C_{\alpha_{Zr}(O)/ox}; X_0^{j+1}(t) = C_{\alpha_{Zr}(O)/\beta_{Zr}}; X_0^j(t) = C_{\beta_{Zr}/\alpha_{Zr}(O)} \quad (12)$$

The coefficients of diffusion of oxygen are defined as constant in each phase given by Eqs. (13)–(15).

$$\forall p \in [1; j] D_0^p = D_{\beta_{Zr}} \quad (13)$$

$$\forall p \in [j+1; i] D_0^p = D_{\alpha_{Zr}(O)} \quad (14)$$

$$\forall q \in [i+1; n] (1+z)D_0^q = D_{oxide} \quad (15)$$

The integration of Fick's laws (Eqs. (3) and (4)) is performed using an algorithm of finite differences. Thus, knowing the variation of concentration of oxygen (or vacancies) in each slab, it is possible to calculate the change in concentration of oxygen (or vacancies) between two time steps Δt , using the Eqs. (16) and (17):

$$\forall p \in [1; i] X_0^p(t + \Delta t) = X_0^p(t) + \Delta t \frac{dX_0^p}{dt} \quad (\text{metal}) \quad (16)$$

$$\forall q \in [i+1; n] X_{V_0}^q(t + \Delta t) = X_{V_0}^q(t) + \Delta t \frac{dX_{V_0}^q}{dt} \quad (\text{oxide}) \quad (17)$$

This algorithm is based on a physical step time δt which satisfies the criteria of convergence of the scheme of the explicit finite differences (Eq. (18)). The normalized time step Δt is linked to δt by the Eq. (19):

$$\delta t \frac{2D_{\max}}{(e_{\min})^2} \leq 1 \quad (18)$$

$$\Delta t = \delta t \frac{(e_{\min})^2}{2D_{\max}} \quad (19)$$

The weight gain per surface can be simply obtained during EKINOX-Zr calculation by integrating the oxygen diffusion profile such as given in Eq. (20):

$$\Delta m = \frac{M_0}{4\Omega_{Zr}} \left(\sum_{p=1}^{i-1} \left[(e^p + e^{p+1}) (X_0^{p+1} + X_0^p) \right] + \frac{\gamma}{\rho} \sum_{q=i+1}^{n-1} \left[(e^q + e^{q+1}) (X_{V_0}^{q+1} + X_{V_0}^q) \right] \right) \quad (20)$$

³ The TQ interface is a set of subroutines and functions which can be used in a program written in FORTRAN as EKINOX-Zr. Thus, the program can perform thermodynamic calculations using ThermoCalc software.

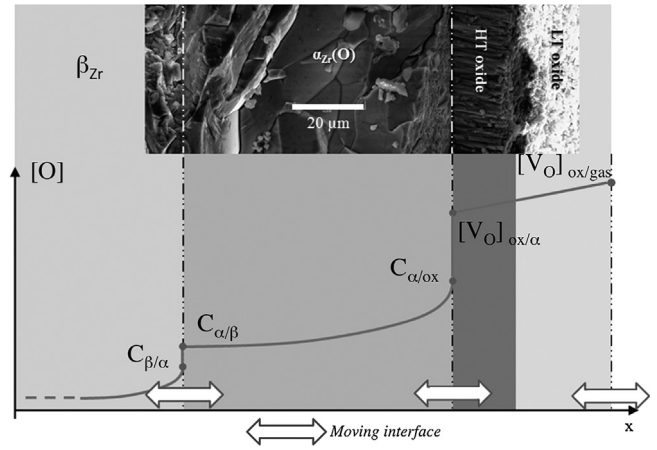


Fig. 2. Top: SEM micrograph (this work) representing a cross section of a prior-oxidized (30 μm) sample of Zircaloy-4 oxidized at 1200 °C under oxygen during 200 s. Bottom: Schematic of the profile of diffusion of oxygen into the fuel cladding tube after oxidation at high temperature.

2.2. EKINOX-Zr modified

Experimental observations of prior-oxidized Zircaloy-4 samples after a high temperature oxidation (Fig. 2) have shown that the oxide layer is divided into two different layers [1]: an outer low temperature oxide layer corresponding to the prior-oxide layer and an inner oxide layer corresponding to the zirconia formed during the high temperature oxidation. Previous simulation results [7] showed that EKINOX-Zr was able to reproduce the phenomenon of reduction/re-growth qualitatively but not quantitatively suggesting that the layer of low temperature zirconia had different diffusion properties at high temperature than the zirconia phase formed at high temperature. Thus, two different hypotheses were tested in the present work in order to obtain a quantitative agreement between calculations and experimental data:

- Hypothesis 1: the two layers of oxide are dense during the whole process but, the properties of diffusion of the $\alpha_{Zr}(O)$ phase formed by reduction of the layer of low temperature oxide are different from those of the $\alpha_{Zr}(O)$ phase formed by transformation of β_{Zr} phase at the $\alpha_{Zr}(O)/\beta_{Zr}$ interface. Moreover, considering the difference between the columnar microstructure of the high temperature oxide layer and the equiaxed microstructure of the low temperature oxide, the oxygen diffusion coefficient of the low temperature oxide layer is set to a lower value than the high temperature oxide one.
- Hypothesis 2: the layer of low temperature oxide is dense during its reduction stage and porous during the inward growth of the layer of high temperature oxide which causes an increase of mechanical stress in the oxide scale because of the high PBR. Then, the oxygen may have a direct access to the inner layer of high temperature oxide.

3. Results

3.1. Numerical simulations

EKINOX-Zr model is able to simulate both oxide and $\alpha_{Zr}(O)$ phase growth kinetics [6–8]. It is also possible to calculate the weight gain due to high temperature oxidation. Many researchers have determined the diffusion coefficient of oxygen in zirconia using different experimental techniques [11–22]. However, a scattering of the diffusion data is observed. In this study, we decided to use the diffusion coefficient of oxygen issued from [22]. As a first

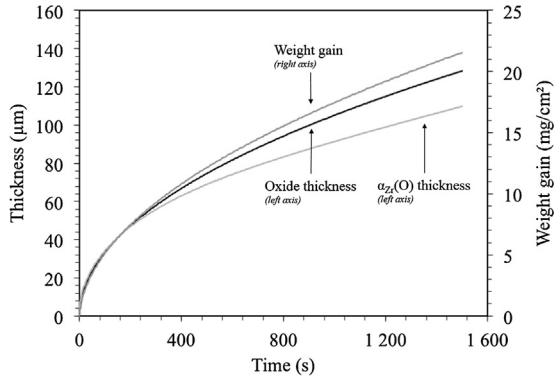


Fig. 3. Weight gain kinetics, oxide growth kinetic and $\alpha_{Zr}(O)$ growth kinetic calculated with EKINOX-Zr for an as-received sample of Zircaloy-4 oxidized during 1500 s at 1200 °C.

Table 1

Input parameters for the simulation of the oxidation at 1200 °C of an as-received sample of Zircaloy-4: kinetic parameters from [20] in (cm²/s) and equilibrium concentrations of oxygen calculated thanks to ThermoCalc and the thermodynamic database Zircobase [9] in (%at).

D_{oxide}	D_{α}	D_{β}	$[V_O]_{ox/\alpha}$	$C_{\alpha/ox}$	$C_{\alpha/\beta}$	$C_{\beta/\alpha}$
$9.36 \cdot 10^{-7}$	$1.10 \cdot 10^{-7}$	$1.55 \cdot 10^{-6}$	6.92	30.5	10.5	2.76

Table 2

Input parameters for the hypothesis 1 (high temperature and low temperature dense layer of oxide and two different layers of $\alpha_{Zr}(O)$): kinetic data from [22] (except D_{LTox} and $D_{\alpha_{red}}$) in (cm²/s), equilibrium concentrations of oxygen calculated with ThermoCalc and the thermodynamic database Zircobase [9] in (%at).

D_{LTox}	D_{HTox}	$D_{\alpha_{red}}$	D_{α}	D_{β}	$[V_O]_{ox/\alpha}$	$C_{\alpha/ox}$	$C_{\alpha/\beta}$	$C_{\beta/\alpha}$
$5.29 \cdot 10^{-7}$	$9.36 \cdot 10^{-7}$	$3.87 \cdot 10^{-8}$	$1.10 \cdot 10^{-7}$	$1.55 \cdot 10^{-6}$	6.92	30.5	10.5	2.76

example, Fig. 3 shows kinetics of growth and the weight gain calculated for an as-received sample of Zircaloy-4 oxidized 1500 s at 1200 °C. The input parameters used for this simulation are reported in Table 1.

As explained in Section 2.2, two different hypotheses have been tested in EKINOX-Zr in order to take into account the presence of a prior-oxide layer formed at low temperature.

3.1.1. Hypothesis 1: dense layer

For this first hypothesis, the layer of low temperature oxide is simply distinguished from the layer of high temperature oxide, considering two distinct coefficients of diffusion. Input parameters used for this simulation are reported in Table 2.

Fig. 4a shows calculated diffusion profiles of oxygen at different times. The evolution of the profile of oxygen with time clearly shows the growth of the layer of $\alpha_{Zr}(O)$ and the increase of the content of oxygen in the β_{Zr} phase. This calculation was performed for a sample of Zircaloy-4 with a prior-oxide layer with a thickness of 30 μm further oxidized 1500 s at 1200 °C. Fig. 4b compares the weight gains calculated for a sample with a prior-oxide and a sample without prior-oxide (as-received) oxidized at high temperature.

3.1.2. Hypothesis 2: porous layer

The hypothesis 2 which considers the oxide formed at low temperature as a porous layer during the high temperature oxide growth process is in accordance with Godlewski's conclusions [23] regarding the porosity of the low temperature oxide. Indeed, Godlewski observed that, during the growth of the layer of zirconia at 360 °C, the Pilling–Bedworth ratio induces compression stresses in the oxide at the metal/oxide interface. The compressive stresses

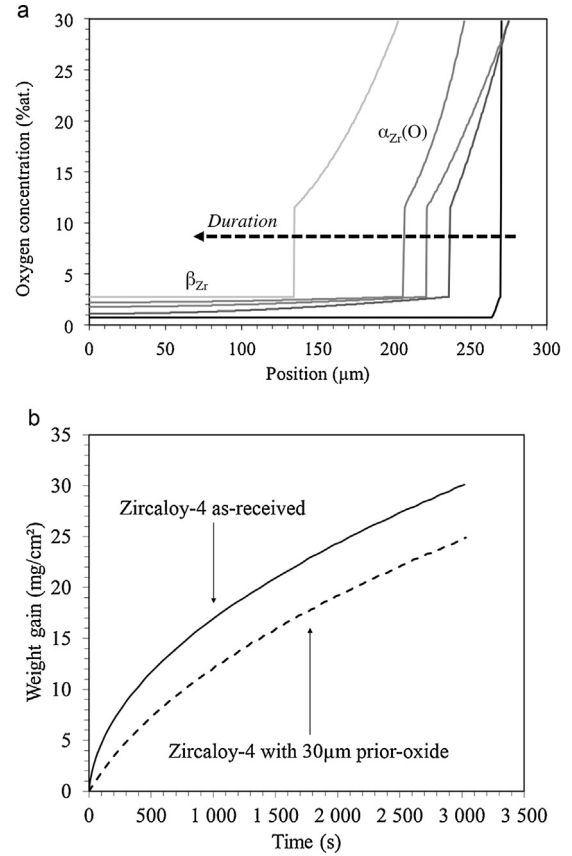


Fig. 4. Hypothesis 1: (a) profiles of diffusion of oxygen calculated with EKINOX-Zr in $\alpha_{Zr}(O)$ phase and β_{Zr} phase for a prior-oxidized (30 μm of prior-oxide) sample of Zircaloy-4 oxidized during 520 s at 1200 °C. (b) Comparison of calculated weight gain as a function of time during oxidation at 1200 °C for an as-received Zircaloy-4 sample and a Zircaloy-4 sample with 30 μm of prior-oxide.

promote the phase transformation monoclinic zirconia to tetragonal zirconia. The oxide layer is a mixture of monoclinic phase (~60%) and of tetragonal phase (~40%). Because of the inward growth mechanism, the maximal stresses are experienced in the inner part of the oxide scale where they stabilize the tetragonal phase. But when this phase moves away from the metal/oxide interface, the stresses are not sufficiently enough to stabilize the tetragonal zirconia and there is a tetragonal to monoclinic phase transformation of the oxide. This phase transformation goes along with a decrease of the molar volume of the oxide and this leads to the appearance of many cracks in the oxide scale. Because of the competition between the displacement of the metal/oxide interface and of the zirconia transformation front (tetragonal to monoclinic), the thickness of the dense oxide layer is quite the same along the oxidation. Following Godlewski's conclusions, the low temperature oxide layer can be more or less considered as porous and in some extreme cases, the oxidizing environment can have a direct access through the low temperature oxide layer. Thus, in a second set of simulations, the hypothesis of a porous layer of low temperature oxide during the growth of the layer of high temperature oxide has been considered (hypothesis 2). This hypothesis is an extreme case. As previous simulations have shown that the experimental reduction stage can be well reproduced considering a dense low temperature oxide layer with a diffusion coefficient of oxygen D_{LTox} equal to $1.09 \cdot 10^{-7}$ cm²/s at 1200 °C, the low temperature oxide is however considered to be dense during the reduction stage. Input parameters used for this simulation are summarized in Table 3.

Fig. 5 shows the growth kinetics and the weight gain calculated using EKINOX-Zr for a prior-oxidized (30 μm of prior-oxide) sample

Table 3

Input parameters for the simulations done with the hypothesis 2 (porous layer of low temperature oxide during growth of the layer of high temperature oxide): kinetic data from [22] (except D_{LTox}) in (cm^2/s), equilibrium concentrations of oxygen calculated with ThermoCalc and the thermodynamic database Zircbase [9] in (%at).

Reduction stage	D_{LTox}	D_{HTox}	D_α	D_β	$[V_O]_{\alpha/\alpha}$	$C_{\alpha/ox}$	$C_{\alpha/\beta}$	$C_{\beta/\alpha}$
	$1.09 \cdot 10^{-7}$	$9.36 \cdot 10^{-7}$	$1.10 \cdot 10^{-7}$	$1.55 \cdot 10^{-6}$	6.92	30.5	10.5	2.76
Oxidation stage	D_{LTox}	D_{HTox}	D_α	D_β	$[V_O]_{\alpha/\alpha}$	$C_{\alpha/ox}$	$C_{\alpha/\beta}$	$C_{\beta/\alpha}$
	$+\infty$	$9.36 \cdot 10^{-7}$	$1.10 \cdot 10^{-7}$	$1.55 \cdot 10^{-6}$	6.92	30.5	10.5	2.76

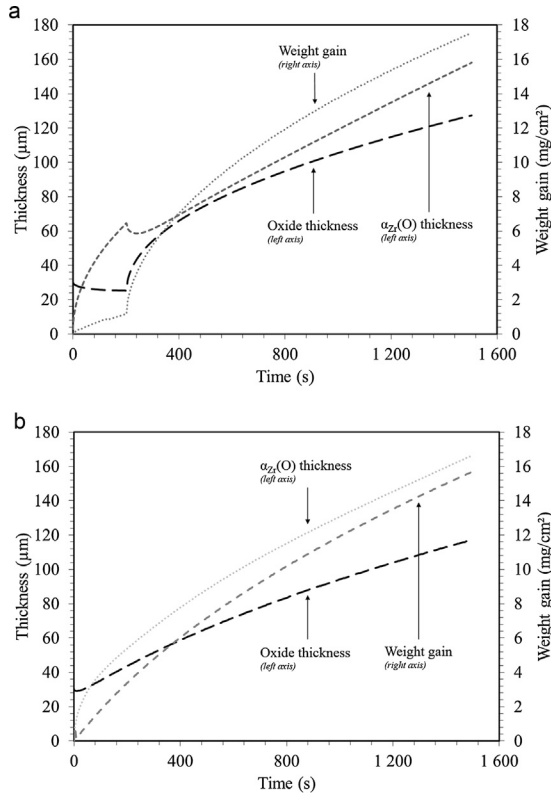


Fig. 5. Kinetics of weight gain, kinetics of growth of the oxide layer and kinetics of growth of $\alpha_{Zr}(O)$ phase calculated for a prior-oxidized sample ($30 \mu\text{m}$ of prior-oxide) of Zircaloy-4 oxidized during 1500 s at 1200°C . (a) Hypothesis 1. (b) Hypothesis 2.

of Zircaloy-4 oxidized during 1500 s at 1200°C for the two hypotheses tested, i.e. a dense (Fig. 5a) or a porous layer of prior-oxide (Fig. 5b). The oxide dissolution stage can be clearly observed on the oxide growth kinetics during the first 170 s (Fig. 5b).

After this stage, the growth of the oxide is rapid as for standard kinetics of an as-received sample (i.e. without prior-oxide). This result is directly linked to the hypothesis of the porous low temperature prior-oxide. The weight gain also exhibits a rapid increase for the same reason. The overall kinetic of growth of the oxide for 1500 s is higher compared to hypothesis 1 (Fig. 5a). In the case of a dense low temperature oxide (hypothesis 1), the stage of reduction of the low temperature prior-oxide also exists but it is very short due to the choice of a higher value for the parameter D_{LTox} . Furthermore, no rapid increase on the weight gain is expected with the first hypothesis. Notice also that the kinetics of growth of the $\alpha_{Zr}(O)$ layer shows a particular behavior in the case of hypothesis 2. A transitory stage of reduction of the whole $\alpha_{Zr}(O)$ thickness starts as soon as the growth of the layer of high temperature oxide begins. This is due to the competition between the displacements of the metal/oxide interface and of the $\alpha_{Zr}(O)/\beta_{Zr}$ interface. When the growth of the layer of high temperature oxide starts, the flux of oxygen in this layer becomes suddenly greater than in the layer of $\alpha_{Zr}(O)$ because of the assumption of a porous layer of low temperature prior-oxide. Consequently, the displace-

Table 4

Data of prior-oxidized samples of Zircaloy-4 used in [1].

Prior-oxide thickness (μm)	[H] (wt. ppm)	Oxidation T ($^\circ\text{C}$)	Oxidation duration (s)
25	500–600	1200	1492
35	750	1200	1492

ment of the metal/oxide interface in favor of the growth of the high temperature oxide is faster than the displacement of the $\alpha_{Zr}(O)/\beta_{Zr}$ interface. This leads to a rapid decrease of the total thickness of the $\alpha_{Zr}(O)$ phase. The flux of oxygen in the layer of high temperature oxide decreases with the thickening of this layer and then the displacement of the metal/oxide interface slows down. As soon as the displacement of the $\alpha_{Zr}(O)/\beta_{Zr}$ interface becomes faster than the displacement of metal/oxide interface, the thickening of the $\alpha_{Zr}(O)$ phase restarts.

In next part, these simulation results will be compared to experimental data.

3.2. Experimental

The effect of a prior-oxide layer on the fuel cladding behavior during LOCA has been studied by several authors. Le Saux et al. [1] have carried out tests under steam oxidation at high temperature on prior-oxidized samples of Zircaloy-4. These layers of prior-oxide with thicknesses of 25 and $35 \mu\text{m}$ had been previously produced in autoclave⁴ at 360°C under an isostatic pressure of $1.9 \cdot 10^7 \text{ Pa}$. The characteristics of these samples (thickness of prior-oxide, content of hydrogen, temperature and duration of the oxidation) are reported in Table 4.

In the present study, samples of Zircaloy-4 were previously oxidized in similar conditions than for the study of Le Saux et al. [1]. Samples were oxidized in an autoclave during 1328 days in order to obtain $30 \mu\text{m}$ of prior-oxide. As for the samples studied in [1], the samples used in this work contained 700 wt. ppm of hydrogen. Then, the effect of hydrogen on the diffusion of oxygen during oxidation at high temperature [1,8,23] was expected to be similar for this work and for the study of Le Saux et al. In this work, the thermal treatments consisted in oxidizing the samples at high temperature in order to reproduce the phenomenon of reduction of the low temperature oxide at four different temperatures, e.g. 1100, 1150, 1200 and 1250°C . The experimental device used to perform the oxidation is composed by two different areas. The first area is a “cold chamber” cooled by a ventilation system; the second area is the furnace where oxidations are performed. The two areas communicate thanks to an alumina tube. The sample is introduced in the cold chamber, then a secondary vacuum is established before filling up the device with a mix gas of $^{18}\text{O}_2/^{16}\text{O}_2$. Then, the sample is introduced in the furnace for the duration of the oxidation. Duration of each oxidation were evaluated before experiments thanks to cal-

⁴ Some B and Li are added in the water of the autoclave to simulate the conditions of the primary circuit of a PWR.

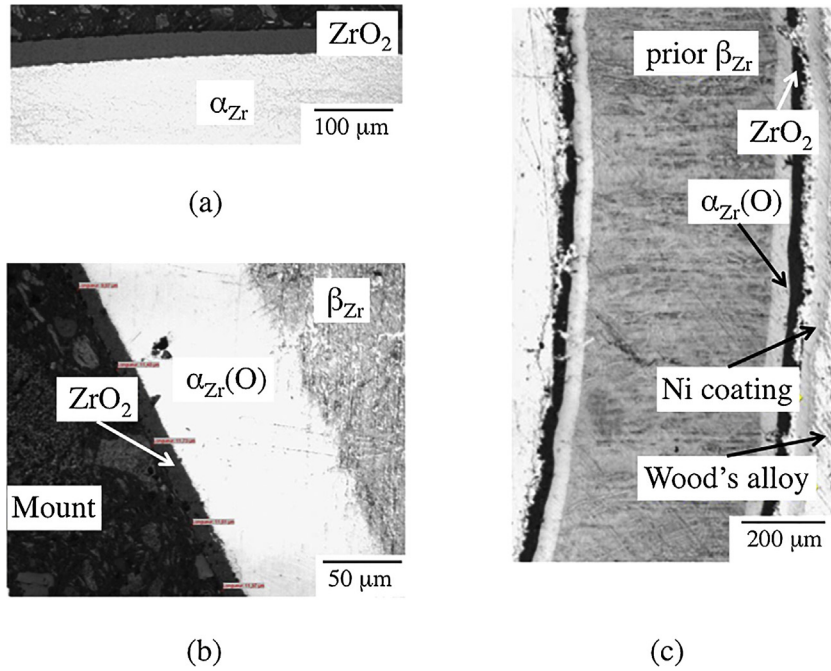


Fig. 6. (a) Optical cross-section of a Zircaloy-4 sample oxidized in autoclave at 360 °C during 1328 days. (b) Optical cross-section of the sample T9 annealed under secondary vacuum of argon at 1200 °C during 510 s. (c) Optical cross-section of the sample T3 oxidized in this work at 1200 °C during 200 s.

Table 5

Temperature and duration of experimental oxidations performed in this study on prior-oxidized (thickness of 30 μm) samples of Zircaloy-4.

Samples	Oxidation temperature (°C)	Oxidation duration (s)
T1	1100	450
T2	1150	280
T3	1200	200
T4	1250	131

calculations with EKINOX-Zr model in order to allow the reduction of the oxide layer. They are listed in Table 5.

Fig. 6 shows three optical cross-sections. The cross-section of the sample issued from the autoclave (Fig. 6a) shows that the low temperature oxide layer formed is 30 μm thick, dense and adherent and the scale thickness appears quite homogeneous. The cross-section of the sample T9, annealed under vacuum at 1200 °C (Fig. 6b), shows that the reduction of the low temperature oxide layer is also homogeneous and the $\alpha_{\text{Zr}}(\text{O})$ phase formed by reduction is quite uniform. The cross-section of the sample T3 oxidized at 1200 °C (Fig. 6c) shows that the metallic layers are quite homogeneous. The scratchy aspect of the two external oxide layers is due to polishing operations.

Thicknesses have been measured thanks to the software Olympus Stream Image Analysis. The average arc length of each sample is around 3.70 cm and we performed forty measurements of each layer along the sample. The measurement of each layer is carried out perpendicularly to both interfaces. The measurement uncertainties were found to be very small compared to the thickness variations.

Fig. 7a and b shows a comparison between experimental and calculated results. First of all, one can see a good agreement between the experimental results from [1] and the present experimental work. Concerning the numerical calculations, the two hypotheses already detailed in a previous section, were tested. In the hypothesis 2, the case of a porous low temperature oxide during the growth of the high temperature oxide layer is considered (Fig. 7 dashed line). For hypothesis 1, dense low temperature and high temperature oxides are considered and a specific coefficient of diffusion of

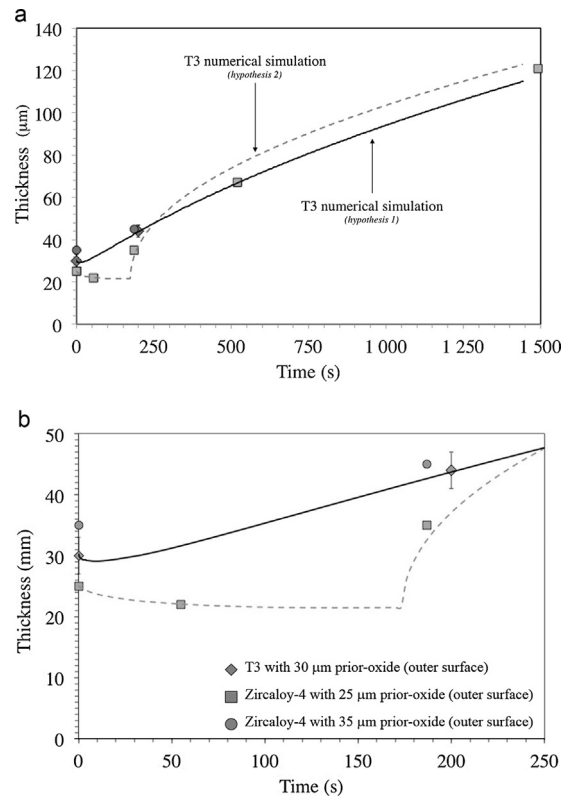


Fig. 7. Comparison between oxide growth kinetics calculated with EKINOX-Zr and experimental data (from this work and [4]). (a) Oxide growth kinetics. (b) Initial oxide growth kinetics between 0 and 250 s. Diamonds: sample T3 oxidized in this work at 1200 °C during 200 s. Squares: samples of Zircaloy-4 with 25 μm thick prior-oxide, oxidized at 1200 °C during 1492 s [1]. Circles: samples of Zircaloy-4 with 35 μm prior-oxide, oxidized at 1200 °C during 187 s [1]. Solid curve: kinetics of growth of oxide calculated with EKINOX-Zr considering hypothesis 1 and a 30 μm thick prior-oxide. Dashed curve: oxide growth kinetics calculated with EKINOX-Zr considering hypothesis 2 and a 25 μm thick prior-oxide.

Table 6

Comparison between experimental weight gains measured after oxidation and weight gains obtained with EKINOX-Zr simulation (hypothesis 1) of the experimental cases.

Samples	Oxidation temperature (°C)	Oxidation duration (s)	Experimental weight gain (mg/cm ²)	Numerical weight gain (mg/cm ²)
T1	1100	450	1.35	1.31
T2	1150	280	1.33	1.36
T3	1200	200	3.42	3.42
T4	1250	131	4.06	4.09

oxygen is attributed to the layer of $\alpha_{Zr}(O)$ formed by reduction of the low temperature oxide (Fig. 7 solid line). The dense low temperature oxide hypothesis reproduced well the experimental results obtained in the present study, whereas it seems that some feature on short time oxidation (50 s) from Le Saux et al. work are better reproduced by the hypothesis of a porous layer of low temperature oxide. However, the exact duration of the dwell at high temperature in case of short time oxidation can be overestimated. More data are needed in order to conclude whether, the first or the second hypothesis is the best.

The weight gains have also been calculated; they are reported in Table 6. A very good agreement is obtained between the calculated and experimental weight gains. Regarding kinetics, it seems that the data from Le Saux et al. for prior-oxidized samples (Fig. 1 in [1]) exhibit a change in the weight gain kinetics after 200 s. This result is consistent with the hypothesis of a dense prior-oxide, i.e. the hypothesis 1 of the present calculations.

Another output of the model is the calculation of thicknesses of the different layers that compose the system: oxide, $\alpha_{Zr}(O)$ and β_{Zr} phases. Except for the oxidation at 1250 °C, one can see that a quite good agreement is also obtained with hypothesis 1 (Table 7) between experimental measurements and simulation results. The lower agreement at 1250 °C can be explained by the faster kinetics at this temperature. Simulations results show smaller amounts of high temperature oxide and $\alpha_{Zr}(O)$ phase in comparison with the experimental data. At 1250 °C, the annealing treatment is shorter and the relative weight of the time needed to introduce the sample in the furnace becomes a source of error.

The behavior of an internal oxide layer (i.e. the oxide layer formed on the internal side of the fuel cladding tube) was also studied. To do so, a sample (T9) with an initial layer of prior-oxide of 30 μm thick was annealed at 1200 °C under secondary vacuum of Ar.⁵ Hence, in these conditions, the thickness of the low temperature oxide layer is reduced at the metal/oxide interface without reaction with the atmosphere and consequently a layer of $\alpha_{Zr}(O)$ phase enriched in oxygen grows. The experimental results confirmed that the thickness of the prior-oxide decreased during the annealing treatment at high temperature without weight change (Table 8). Numerical calculations have been performed with the EKINOX-Zr model in order to reproduce this phenomenon considering a dense layer of low temperature oxide. The comparison between numerical results (hypothesis 1) and experimental ones from this work and from [1] are presented in Fig. 8. They show a very good agreement. The numerical calculation results stand between the experimental points issued from [1] for samples of Zircaloy-4 with a prior-oxide (respectively 25 and 35 μm of prior-oxide).

Finally, Fig. 9 presents the variation of the thickness of the oxide layer as a function of time for the four different temperatures of oxidation tested. The hypothesis of two dense layers of oxide (i.e. hypothesis 1) allows reproducing correctly the experimental data.

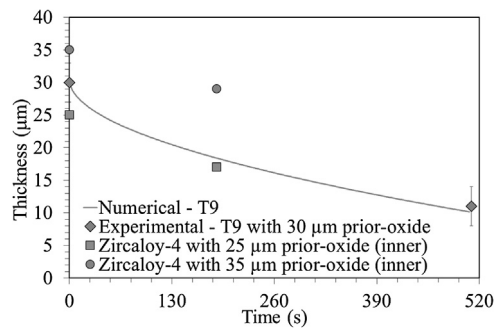


Fig. 8. Experimental results (diamonds) and numerical result obtained with EKINOX-Zr (curve) for sample T9. Experimental results extracted from [1] for samples of Zircaloy-4 with 25 and 35 μm of prior-oxide. All those samples have been annealed under secondary vacuum of argon at 1200 °C during 510 s (in case of sample T9) and 187 s (sample from [4]).

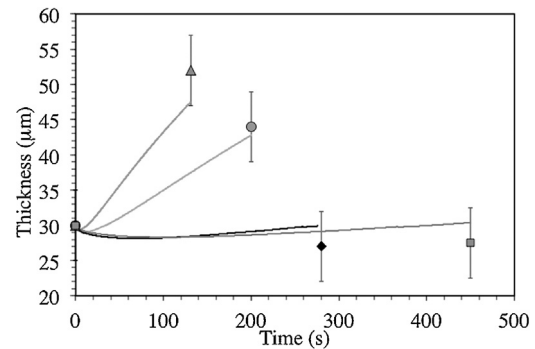


Fig. 9. Comparison between experimental results (dots) and those obtained with EKINOX-Zr (curves). All the samples had a prior-oxide layer of 30 μm before the oxidation at high temperature. T1: oxidized 450 s at 1100 °C. T2: oxidized 280 s at 1150 °C. T3: oxidized 200 s at 1200 °C. T4: oxidized 131 s at 1250 °C.

4. Discussion

Results show that experimental data can be reproduced by the EKINOX-Zr model considering the hypothesis 1 (two dense layers of oxide) or the hypothesis 2 (porous layer of low temperature oxide during growth at high temperature) and with different properties of diffusion in the $\alpha_{Zr}(O)$ phase depending on the phase from which it was formed. Hypothesis 2 of a porous layer of low temperature oxide is quite extreme. It can be supposed that the changeover from dissolution to regrowth of the oxide scale leads to a particular stress state evolution of the remaining low temperature oxide. Indeed, the dissolution/regrowth step induces a change for the interface metal/oxide displacement from one direction to the other, which is not often reported in the literature. The huge change of molar volume associated with the dissolution of the oxide at the constrained metal/oxide interface (with the circular shape of the cladding) and, later, the transformation strain due to the re-oxidation of this area, leads to a particular loading which could damage the low temperature oxide scale when the high temperature oxide scale growth began.

Thus the oxidizing gas can have a direct access to the LT oxide/HT oxide interface. But, this porous character may change along the sample as a function of the reduction rate of the layer of low temperature oxide. Then, experiments and micro characterizations must be performed to evaluate this porosity. On the contrary, hypothesis 1 differentiates the layer of $\alpha_{Zr}(O)$ formed by reduction of the layer of low temperature oxide from the layer formed by transformation of the β_{Zr} phase. This hypothesis shows a good agreement between experimental data (from this work and from [1]) and numerical simulations (Figs. 7 and 8) using the coefficients of dif-

⁵ i.e. the furnace was filled with Ar before to establish a secondary vacuum and a small input flux of Ar was used to regulate the pressure.

Table 7

Experimental thicknesses of layers measured on the external half of each sample, compared with numerical thicknesses obtained with the hypothesis 1 (note that for samples oxidized at 1100 and 1150 °C, it is not possible to distinguish experimentally the layer of low temperature oxide from the layer of the high temperature oxide).

Samples	Oxidation T (°C)	Oxidation time (s)	Types	Oxide thickness (μm)		α _{Zr} (O) thickness (μm)	β _{Zr} thickness (μm)
T1	1100	450	Exp.	27 ± 2		49 ± 6	220 ± 7
			Num.	30			
T2	1150	280	Exp.	26 ± 3		36 ± 11	219 ± 2
			Num.	31			
T3	1200	450	Exp.	LT	HT	44 ± 4	219 ± 2
			Num.	28 ± 2	16 ± 3		
T4	1250	131	Exp.	29	14	42	221
			Num.	20 ± 2	32 ± 2		
				29	20	40	220

Table 8

Comparison between experimental and numerical (hypothesis 1) weight gain of the T9 sample (dissolution of the prior-oxide layer into the alloy under Ar secondary vacuum at 1200 °C during 510s). Thicknesses of phases were measured on the external half of the T9 sample.

Sample	Reduction time and temperature	Types	Weight gain (mg/cm ²)	Oxide thickness (μm)	α _{Zr} (O) thickness (μm)	β _{Zr} thickness (μm)
T9	510 s	Exp.	0.00 ± 0.02	11 ± 1	88 ± 8	189 ± 4
	1200 °C	Num.	0.00 ± 0.02	12	88	189

fusion of oxygen reported in Table 2. One can see that $D_{LT_{tox}}$ is lower than $D_{HT_{tox}}$, the same observation can be done for $D_{\alpha_{red}}$ and D_{α} . High temperature and low temperature zirconia scales are clearly identified on our samples by the difference of microstructures. According to SEM observations (Fig. 2) the microstructure of the layer of low temperature oxide is composed of equiaxed grains whereas the high temperature oxide is composed by columnar grains. The high temperature zirconia is also reported as large columnar grain microstructure in literature. The columnar morphology of the high temperature oxide with columns perpendicular to the sample surface may promote the diffusion of the oxygen through this oxide scale compared to the low temperature oxide microstructure made of equiaxed grains. At low temperature oxide scale formed on Zircaloy-4 is reported to be composed of a mixture of columnar and equiaxed grains [24]. The columnar grains have monoclinic structure and are usually referred as the protective part of the oxide scale at low temperature. However during the high temperature treatment the phase transformation occurs in monoclinic zirconia to tetragonal and only equiaxed grains are maintained for the low temperature zirconia microstructure. There is no data on the diffusion coefficient of oxygen in the low temperature oxide layer formed at 360 °C and then heated up to 1200 °C to compare it to value estimated in our study. In the case of the layer of α_{Zr}(O), the reduction of the low temperature oxide could form an α_{Zr}(O) phase over-saturated in oxygen which induces a deformation of the crystallographic structure and a saturation of the interstitial sites. The properties of diffusion of this HCP α_{Zr} phase over-saturated in oxygen are not known. The good agreement obtained between numerical simulations and experimental data shows that taking into account two dense layers of oxide and the change of the properties of diffusion in the α_{Zr}(O) phase with saturation in oxygen allows a good simulation of the phenomenon of reduction/re-growth.

The reduction/re-growth occurrence depends on the thickness of the prior-oxide on the sample just before the high temperature annealing. Fig. 10 shows the kinetics of growth of the oxide layer calculated at 1200 °C by EKINOX-Zr considering different thicknesses of prior-oxide. These simulations show that the phenomenon of reduction/re-growth is only observed for a thickness of prior-oxide higher than 10 μm. Indeed, when the thickness of prior-oxide is smaller than 10 μm, the flux of oxygen in the low temperature oxide layer remains always higher than the flux of oxygen in the α_{Zr}(O) phase. Thus, there should be no decrease of the low temperature oxide layer thickness in this latter case, according to modeling of the phenomenon.

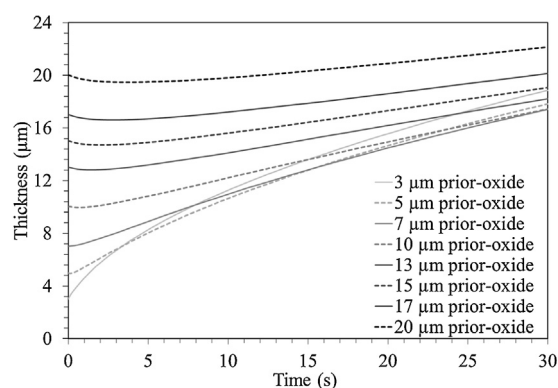


Fig. 10. Calculated growth kinetics of oxide at 1200 °C for samples of Zircaloy-4 with different thicknesses of prior-oxide.

The model developed in the present work allows calculating the kinetics of oxygen ingress in the system. Oxygen is a source of embrittlement for the HCP α_{Zr} phase [6,25–28], as it is the case for titanium-base alloys with the α_{Ti} phase [29]. In the present case, when the sample is cooled down from the high temperature, it is composed of an external α_{Zr} layer which was enriched in oxygen at high temperature, and an inner α_{Zr} layer which was formed during cooling by transformation of the prior-β_{Zr} phase. At high temperature, the β_{Zr} phase dissolved much less oxygen than the outer α_{Zr} layer. If we take—for illustration—the value of 0.4(±0.1) %wt, determined by Brachet et al. [30], as the maximum oxygen content for the prior-β_{Zr} phase to be ductile at room temperature, we can perform simulations to evaluate the variation of the remaining thickness of the prior-β_{Zr} phase containing less than 0.4 %wt after high temperature oxidation. This was done as a function of temperature and for several thicknesses of prior-oxide. The remaining thickness of ductile prior-β_{Zr} phase was evaluated as the thickness of the prior-β_{Zr} where the oxygen concentration is lower than the value determined by Brachet et al. [30] at room temperature. This critical concentration of oxygen was taken as an example and should not be considered as an absolute value. Indeed, this value was determined at room temperature but it is important to notice that after cooling of the vessel in the LOCA scenario, the temperature of the reactor core is close to 100 °C and not 20 °C. Garde and Kassner [31] performed analysis à 100 °C and they found that concentration of oxygen of the ductile-to-brittle transition of the β_{Zr} is between 0.6 %wt and 0.7 %wt. This range is consistent with

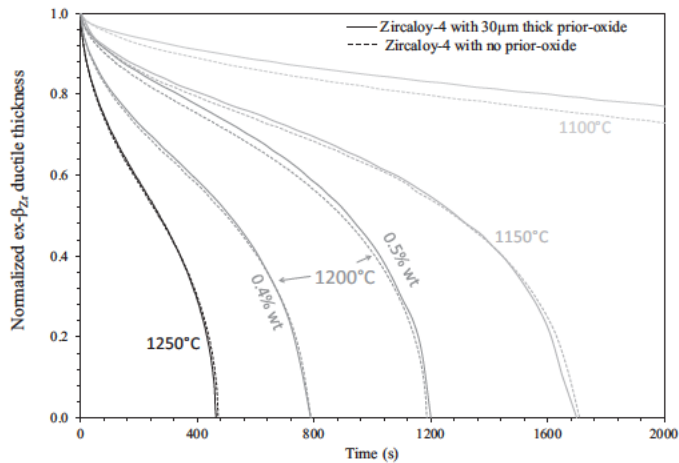


Fig. 11. Variation of the remaining prior- β_{Zr} layer thickness containing less than 0.4%wt of oxygen (and $[O] < 0.5\%$ wt for 1200°C) as a function of time for different temperatures of the high temperature dwell in LOCA conditions. Calculations are made for samples of Zircaloy-4 oxidized on a single face, with and without prior-oxide formed at low temperature during in service conditions. The remaining thickness of the prior- β_{Zr} phase is normalized to the initial thickness (before the high temperature dwell) of β_{Zr} phase.

the results of Sawatzky's study [32]. A higher oxygen content limit when increasing the testing temperature after oxidation, leads to a thicker remaining ductile β_{Zr} . The main objective of these last simulations was to qualitatively evaluate the effect of the prior-oxidation on the ingress of oxygen and possibly on the residual ductility of the fuel cladding after LOCA. Calculations have been made considering Zircaloy-4 fuel cladding tube with an initial wall-thickness of 570 μm . Since the initial thickness of the β_{Zr} phase differs between samples with or without a prior-oxide layer, Fig. 11 shows the evolution of the thickness of the ductile layer of prior- β_{Zr} phase (which contained less than 0.4%wt of oxygen and is then expected to be ductile at room temperature after high temperature oxidation) normalized to the initial (i.e. before oxidation at high temperature) thickness of the layer of β_{Zr} for each case. Comparisons are shown for oxidations performed at 1100, 1150, 1200 and 1250°C for as-received and prior-oxidized (30 μm of prior-oxide) samples of Zircaloy-4. Fig. 11 clearly shows that the evolution with time of this prior- β_{Zr} layer poor in oxygen is strongly influenced by the temperature of oxidation. These calculations confirm the conclusions of Le Saux et al. [1] from their experimental works. They enable to visualize the consequences of a prior-oxidation for any oxidation temperatures and any prior-oxidized thicknesses. Hence, for short oxidation times, post-quench ductility of prior-oxidized samples oxidized between 1250 and 1100°C is close to that of as-received samples (prior-hydrided at an equivalent content of hydrogen) oxidized under similar conditions. EKINOX-Zr calculations confirm that the non-protective effect of prior-oxide layers regarding post-quench mechanical properties is due to the fact that the overall quantity of oxygen atoms diffusing into the sub-oxide metallic layers at high temperature does not depend on the source of oxygen (reduction of the prior-oxide or formation of a "fresh" oxide). From these first calculations, the impact of the prior-oxide on the evolution of the thickness of β_{Zr} ductile phase is low at all temperatures between 1250 and 1100°C. This can be evaluated by comparing the two curves obtained at 1200°C with a critical concentration in oxygen of 0.4%wt and 0.5%wt, these values being typical of the experimental uncertainty on the ductile-brittle transition limit at room temperature. It can be seen on Fig. 11, that the difference between these two curves is much larger than the difference between the curves for the sample with or without a prior-oxide.

5. Conclusion

The aim of this work was to understand and simulate the phenomenon of reduction/re-growth of the oxide layer that was experimentally observed during the oxidation at high temperature of samples of Zircaloy-4 with a thick prior-oxide. This work was based on simulations and experimental results on the oxidation at high temperature of samples of Zircaloy-4 with a thick prior-oxide. Simulations consisted in calculations performed with EKINOX-Zr model which is based on 1D numerical resolution of diffusion-reaction equations describing the diffusion of oxygen in the $\text{ZrO}_2/\alpha_{Zr}(\text{O})/\beta_{Zr}$ system. In a previous work [5], it was shown that the experimental data cannot be reproduced by simulations done with an assumption of a unique and constant coefficient of diffusion of oxygen in each of the three phases. This previous result suggested that the layer of low temperature oxide may have different properties of diffusion than the layer of high temperature oxide. Then, in the present study, a set of new simulations considering two different layers of zirconia (low temperature and high temperature oxide layers) was performed and new experimental data were obtained on samples of Zircaloy-4 with a prior-oxide thickness of 30 μm . These later experimental data are in quite good agreement with Le Saux et al. study [1] on samples of Zircaloy-4 with a thickness of prior-oxide respectively equal to 25 μm and 35 μm thick for a larger time range of oxidation. The new experimental results were compared with EKINOX-Zr calculations performed with two different hypotheses, a porous or dense layer of low temperature oxide as well as new assumption for the α_{red} phase. Simulations well reproduced the experimental evolutions of the thickness of the different phases. First, this result confirms that the properties of diffusion of the low temperature oxide are strongly different from the high temperature oxide ones. However, considering the experimental uncertainty, none of the two hypotheses (porous or dense low temperature zirconia) can be definitively excluded. Forthcoming ^{18}O tracers experiment should bring some helpful information on the properties of diffusion at high temperature of the layer of zirconia prior-oxide grown at low temperature.

Second, a specific coefficient of diffusion was attributed to the $\alpha_{Zr}(\text{O})$ phase growing at the oxide/metal interface from the reduction of low temperature oxide. It was considered that this phase should have different properties of diffusion with respect to the $\alpha_{Zr}(\text{O})$ phase that grows at the α phase that grows at the $\alpha(\text{O})/\beta_{Zr}$ interface from a metallic parent phase. Calculations show that the part of $\alpha_{Zr}(\text{O})$ phase that grows from low temperature oxide reduction disappears after a short time because the fast kinetics of regrowth of the high temperature oxide at the metal/oxide interface. However experiments should be done in order to evaluate the evolution of the coefficient of diffusion of oxygen with its own concentration in $\alpha_{Zr}(\text{O})$ phase in order to improve the accuracy of the simulations.

Last, it was shown that the model can be used to anticipate post-quenched mechanical properties of the material oxidized at high temperature, after prior-oxidation or not, if the concentration in oxygen under which the β_{Zr} phase remains ductile is known. Nevertheless a quantitative prediction of the thickness of the remaining ductile layer is difficult due to its high sensitivity to the critical content in oxygen taken for the ductile to brittle transition. Furthermore, the effect of prior-oxide is within experimental uncertainty.

Acknowledgements

The authors want to thank Laurent FAYETTE and Joël GODLEWSKI who performed the oxidation of samples Zircaloy-4 in autoclave at CEA center of Cadarache. They also want to thank Jean-Christophe BRACHET and Matthieu LE SAUX for their helpful

advices. Finally, they want to thank AREVA NP and EDF for their financial and material support and for useful discussions.

References

- [1] M. Le Saux, J.-C. Brachet, V. Vandenberghe, D. Gilbon, J.-P. Mardon, B. Sebbari, Influence of a pre-transient oxide on LOCA high temperature steam oxidation and post-quench mechanical properties of Zircaloy-4 an M5™ cladding, in: Proceedings of 2011 Water Reactor Fuel Performance Meeting, September 11–14, Paper T3-04, Chengdu, China, 2011.
- [2] J.-C. Brachet, V. Vandenberghe, Letter to the editor, J. Nucl. Mater. 395 (2009) 169–172.
- [3] S. Leistikow, G. Schanz, H. van Berg, Kinetik und morphologie der isotherm dampf-oxidation von Zircaloy-4 bei 700–1300 °C, KfK 2587 (1978).
- [4] T. Chuto, F. Nagase, T. Fuketa, High temperature oxidation of Nb-containing Zr alloy cladding in LOCA conditions, Nucl. Eng. Technol. 41 (2009) 163–170.
- [5] S. Guilbert, P. Lacote, G. Montigny, C. Duriez, J. Desquines, C. Grandjean, Effect of pre-oxide on Zircaloy-4 high temperature steam oxidation and post-quench mechanical properties Zirconium in the Nuclear Industry, vol. 17, ASTM, International, 2015, pp. 952–978, ASTM STP1543.
- [6] B. Mazères, Étude Expérimentale et Modélisation de l'Oxydation à Haute Température et des Transformations de Phases Associées Dans les Gains en Alliage de Zirconium. PhD Thesis, Université de Toulouse, 2013 <http://ethesis.inp-toulouse.fr/archive/00002751>.
- [7] C. Toffolon-Masclat, C. Desgranges, C. Corváln-Moya, J.-C. Brachet, Simulation of the $\beta_{Zr} \rightarrow \alpha_{Zr}(O)$ phase transformation due to oxygen diffusion during high temperature oxidation of zirconium alloys, Solid State Phenom. 172–174 (2011) 652–657.
- [8] B. Mazères, C. Desgranges, C. Toffolon-Masclat, D. Monceau, Contribution to modeling of hydrogen effect on oxygen diffusion in Zircaloy-4 alloy during high temperature steam oxidation, Oxid. Met. 79 (2013) 121–133.
- [9] N. Dupin, I. Ansara, C. Servant, C. Toffolon, C. Lemaignan, J.-C. Brachet, A thermodynamic database for zirconium alloy, J. Nucl. Mater. 275 (1999) 287–295.
- [10] C. Wagner, Beitrag zur theorie des anlaufvorgangs, Zeitschrift für Physik B21 (1993) 25.
- [11] B. Oberländer, P. Kofstad, I. Kvernes, On oxygen diffusion in tetragonal zirconia, Materialwissenschaft Werkstofftechnik 19 (1988) 190–193.
- [12] R.E. Pawel, Oxygen diffusion in the oxide and alpha phases during reaction of Zircaloy-4 with steam from 1000° to 1500 °C, J. Electrochem. Soc. 126 (1979) 1111–1118.
- [13] V.V. Kharton, E.M. Naumovitch, A.A. Vecher, Research on the electrochemistry of oxygen ion conductors in the former Soviet Union. I. ZrO₂-based ceramic materials, J. Solid State Electrochem. 3 (1999) 61–81.
- [14] M. de Ridder, R.G. van Welzenis, H.H. Brongersma, U. Kreissig, Oxygen exchange and diffusion in the near surface of pure and modified yttria-stabilised zirconia, Solid State Ion. 158 (2003) 67–77.
- [15] P.S. Manning, J.D. Sirman, R.A. De Souza, J.A. Kilner, The kinetics of oxygen transport in 9.5 mol% single crystal yttria stabilised zirconia, Solid State Ion. 100 (1997) 1–10.
- [16] N. Sakai, Y.P. Xiong, K. Yamaji, H. Kishimoto, T. Horita, M.E. Brito, H. Yokokawa, Transport properties of ceria-zirconia-yttria solid solutions $\{(CeO_2)_x(ZrO_2)_{1-x}\}_{1-y}(YO_{1.5})_y$ ($x = 0-1$ $y = 0.2, 0.35$), J. Alloys Compd. 408–412 (2006) 503–506.
- [17] H. Anada, B.J. Herb, K. Nomoto, S. Hagi, R.A. Graham, T. Kuroda, Effect of annealing temperature on corrosion behavior and ZrO₂ microstructure of Zircaloy-4 cladding tube, Zirconium in the Nuclear Industry: 11th International Symposium, ASTM, International, STP1295 (1996) 74–93.
- [18] D. Pêcheur, J. Godlewski, P. Billot, J. Thomazet, Microstructure of oxide films formed during the waterside corrosion of the Zircaloy-4 cladding in lithiated environment, Zirconium in the Nuclear Industry: 11th International Symposium, ASTM, International, STP1295 (1996) 94–113.
- [19] B. Cox, J.P. Pemsler, Diffusion of oxygen in growing zirconia films, J. Nucl. Mater. 28 (1968) 73–78.
- [20] S. Chevalier, Diffusion of oxygen in thermally grown oxide scales, Defect Diffus. Forum 289–292 (2009) 405–412.
- [21] J. Debuigne, Contribution à l'étude de l'Oxydation du Zirconium et de la Diffusion de l'Oxygène dans l'Oxyde et dans le Métal. PhD Thesis, Paris, 1966.
- [22] X. Ma, C. Toffolon-Masclat, T. Guilbert, D. Hamon, J.-C. Brachet, Oxidation kinetics and oxygen diffusion in low-tin Zircaloy-4 up to 1523 K, J. Nucl. Mater. 377 (2008) 359–369.
- [23] J. Godlewski, Oxydation d'Alliages de Zirconium en Vapeur d'Eau: Influence de la Zirconie Tétraogonale sur le Mécanisme de Croissance de l'Oxyde, PhD Thesis, University of Technology of Compiègne, 1990.
- [24] A. Yilmazbayhan, A.T. Breval, R.J.C. Motta, Transmission electron microscopy examination of oxide layers formed on Zr alloys, J. Nucl. Mater. 349 (2006) 265–281.
- [25] J.-C. Brachet, V. Vandenberghe, L. Portier, D. Gilbon, A. Lesbros, J.-P. Mardon, Hydrogen content, pre-oxidation and cooling scenario effects on post-quench microstructure and mechanical properties of Zircaloy-4 an M5™ alloys in LOCA conditions, J. ASTM Int. 5 (2008) 28, Paper ID: JA1101116.
- [26] J.-C. Brachet, V. Vandenberghe, L. Portier, A. Stern, D. Gilbon, J.-P. Mardon, B. Hafidi, A. Pineau, Effets des transformations de phases sur le comportement mécanique d'alliages base zirconium, pendant et après incursion à haute température en ambiance oxydante (vapeur), Matériaux Techniques 97 (2009) 89–98.
- [27] J.H. Kim, M.H. Lee, B.K. Choi, Y.H. Jeong, Failure behavior of Zircaloy-4 cladding after oxidation and water quench, J. Nucl. Mater. 362 (2007) 36–45.
- [28] F.C. Iglesias, D.B. Duncan, S. Sagat, H.E. Sills, Verification of the FROM model for Zircaloy oxidation during high temperature transients, J. Nucl. Mater. 130 (1985) 36–44.
- [29] W. Jia, W. Zeng, J. Liub, Y. Zhou, Q. Wang, Influence of thermal exposure on the tensile properties and microstructures of Ti60 titanium alloy, Mater. Sci. Eng. A 530 (2011) 511–518.
- [30] J.-C. Brachet, J. Pelchat, D. Hamon, R. Maury, P. Jacques, J.-P. Mardon, Mechanical behavior at room temperature and metallurgical study of low-tin Zircaloy-4 and M5™ after oxidation at 1100 °C and quenching, in: Proceeding of the Technical Committee Meeting: Fuel Behavior Under Transient and LOCA Conditions, Halden, Norway, 2001.
- [31] A.M. Garde, T.F. Kassner, Instrumented Impact Properties of Zircaloy-oxygen and Zircaloy-hydrogen Alloys, ANL-80-14, NUREG/CR-1408 (1980).
- [32] A. Sawatzky, A proposed criterion for the oxygen embrittlement of Zircaloy-4 fuel cladding, Zirconium in the Nuclear Industry: 4th International Symposium, ASTM, International (1979) 479–496, ASTM STP681.

Glossary of symbols

- J_0^p : is the oxygen flux from the slab $p + 1$ to the slab p
 $J_{V_0}^q$: is the vacancies flux from the slab $q + 1$ to the slab q
 D_0^p : is the oxygen diffusion coefficient in the slab p
 $D_{V_0}^q$: is the vacancies diffusion coefficient in the slab q
 X_0^p : is the oxygen concentration in the slab p
 $X_{V_0}^q$: is the vacancies concentration in the slab q
 e^p : is the thickness of the slab p
 Ω^p : is the molar volume of the slab p
 z : is the electrical charge of anionic vacancies
 \dot{X}_0^p : is the variation velocity of the oxygen concentration in the slab p
 $\dot{X}_{V_0}^q$: is the variation velocity of the anionic vacancy concentration in the slab q
 P : is the Pilling–Bedworth ratio which is equal to 1.56 in the case of the zirconium/zirconia system
 γ : is the stoichiometric subscript of the oxide MO_γ , γ is equal to 2 for the zirconia
 $[V_0]_{ox/gas}$: is the equilibrium anionic vacancy concentration at the oxide/gas interface in the oxide
 $[V_0]_{ox/\alpha_{Zr}(O)}$: is the equilibrium anionic vacancy concentration at the oxide/metal interface in the oxide
 $C_{\alpha_{Zr}(O)/\alpha_{Zr}}$: is the equilibrium oxygen concentration at the oxide/metal interface in the metal
 $C_{\alpha_{Zr}(O)/\beta_{Zr}}$: is the equilibrium oxygen concentration at the $\alpha_{Zr}(O)/\beta_{Zr}$ interface in the $\alpha_{Zr}(O)$ phase
 $C_{\beta_{Zr}/\alpha_{Zr}(O)}$: is the equilibrium oxygen concentration at the $\alpha_{Zr}(O)/\beta_{Zr}$ interface in the β_{Zr} phase
 $D_{\beta_{Zr}}$: is the oxygen diffusion coefficient in β_{Zr} phase
 $D_{\alpha_{Zr}(O)}$: is the oxygen diffusion coefficient in $\alpha_{Zr}(O)$ phase
 D_{oxide} : is the oxygen diffusion coefficient in zirconia
 δt : is the physical time step
 Δt : is the numerical time step
 D_{max} : is the maximum oxygen diffusion coefficient in the model
 e_{min} : is the minimal thickness of a slab
 Δm : is the weight gain per surface unit
 M_O : is the molar mass of oxygen
 Ω_{Zr} : is the molar volume of zirconium